Published in final edited form as:
Nat Methods. 2019 April 1; 16(6): 526–532. doi:10.1038/s41592-019-0421-z.

Bioluminescent-based imaging and quantification of glucose uptake *in vivo*

Tamara Maric[#1], **Georgy Mikhaylov**[#1,$], **Pavlo Khodakivskyi**[1], **Arkadiy Bazhin**[1], **Riccardo Sinisi**[1], **Nicolas Bonhoure**[2], **Aleksey Yevtodiyenko**[1], **Anthony Jones**[3], **Vishaka Muhunthan**[3], **Gihad Abdelhady**[3], **David Shackelford**[3], and **Elena Goun**[1,*]

[1]Institute of Chemical Sciences and Engineering (ISIC), Swiss Federal Institute of Technology (EPFL), Lausanne, Switzerland [2]Nestlé Institute of Health Sciences SA, EPFL Innovation Park, Bâtiments G/H, Lausanne, Switzerland [3]Department of Pulmonary and Critical Care Medicine, David Geffen School of Medicine, University of California, Los Angeles, California, USA

[#] These authors contributed equally to this work.

Abstract

Glucose is a major source of energy for most living organisms and its aberrant uptake is linked to many pathological conditions. However, our understanding of disease-associated glucose flux is limited due to the lack of robust tools. To date, positron emission tomography (PET) imaging remains the gold standard for measuring glucose uptake, and no optical tools exist for non-invasive longitudinal imaging of this important metabolite in *in vivo* settings. Here we report the development of a novel bioluminescent glucose uptake probe (BiGluc) for real-time, non-invasive longitudinal imaging of glucose absorption both *in vitro* and *in vivo*. In addition, we demonstrate that the sensitivity of our method is comparable with commonly used ^{18}F-FDG-PET tracers and validate BiGluc as a tool for the identification of novel glucose transport inhibitors. The new imaging reagent enables a wide range of applications in the field of metabolism and drug development.

[*]correspondence should be addressed to E.G. (elena.goun@epfl.ch).
[$]current address: Jožef Stefan Institute, Jamova cesta 39, Ljubljana, Slovenia

Data availability statement
The data that support the findings of this study are available from the corresponding author upon request.

Author contributions
E.G. conceptualized the study. I*n vitro* and *in vivo* experiments (except PET study) were carried out by T.M., G.M. (Fig. 3 a-c), P. K., R.S., A.B., A.Y., and N.B. (Fig. 2 e),. P.K. and R.S. synthesized CLP and various GAz reagents. T.M. and A.B. carried out reaction kinetic studies. D.S., A.J., V.M., and G.A., designed and performed PET imaging experiments. E.G., T.M. and G.M. wrote the manuscript and A.Y., P. K., R.S., A.B., N.B., and D.S. edited the manuscript. E.G. acquired the funding.

Competing interests
Authors declare no competing interest.

Europe PMC Funders Author Manuscripts

Introduction

Glucose is the primary energy source for most organisms, used in both aerobic and anaerobic respiration. Impaired glucose consumption is one of the principle markers for various disease conditions, including cancer, diabetes, and obesity1–3. Thus, the ability to noninvasively assess glucose utilization is of high interest. Several techniques have been developed to selectively image and quantify glucose uptake4–7, with positron emission tomography (PET) remaining the most common for measuring glucose uptake in clinical and preclinical settings8. However, it is not easily applicable in laboratory settings because of the short half-life of the reagent (110 min), the necessity of an on-site cyclotron, high cost, and the exposure of personnel to ionizing radiation.

The major shortcomings of ^{18}F-FDG radionuclide imaging motivated the development of non-radioactive chemical tools for probing glucose uptake. These non-radioactive methods include hyperpolarized MRI (^{13}C-labeled D-glucose), stimulated Raman scattering, mass spectrometry, and fluorescent optical imaging4–7. Optical imaging reagents remain among the most prominent because they complement microscopy-based cell imaging and are cost-effective, convenient to use, and offer a high-throughput alternative to all other modalities in a preclinical setting5, 9. Reagents such as fluorescent 2-deoxy-glucose analogs, 2-NBDG10 and 6-NBDG11, were developed and used in various imaging studies monitoring glucose uptake via GLUT, though they absorb and emit light in green wavelengths that are not optimal for detecting signals from living tissues. Therefore, their application *in vivo* is associated with weak fluorescence intensity, high background autofluorescence, low tissue penetration (<1 mm), and high dosage requirements6. To improve signal penetration in tissues, near-infrared fluorescent 2-deoxy-D-glucose conjugates (NIR 2-DG), have recently been reported12–14. However, due to the large size of NIR fluorophores (MW 600-700) in comparison to glucose (MW 180.16), these molecules do not mimic naturally-occurring GLUT-mediated glucose flux9, 12.

To develop sensitive, non-radioactive, and easy-to-use optical tools to image glucose uptake non-invasively *in vitro* and *in vivo*, we chose bioluminescent imaging (BLI). BLI has a high sensitivity, an outstanding signal-to-noise ratio, and favorable properties for non-invasive *in vivo* imaging15–17. It works by exploiting luciferase catalyzed light production *via* the oxidation of small molecule substrates (luciferins) when the enzyme is expressed as a reporter15. While multiple luciferase-expressing animal models of human diseases have been recently reported and even commercially available15, 16, the applications of BLI techniques for the *in vivo* imaging of metabolic uptake remain limited4, 15, 18.

In this study, we present a novel BLI-based optical imaging reagent for the non-invasive imaging and quantification of glucose uptake, named the "bioluminescent glucose uptake probe" (BiGluc). Our findings demonstrate that BiGluc can reliably measure glucose uptake in living cells and that this technology is more sensitive than other commonly used fluorescence-based techniques *in vitro*. In addition, BiGluc can successfully image and quantify metabolic fluxes of glucose in living mice in a non-invasive and longitudinal fashion and a detectable signal is observed even in the deep organs of living animals, such as the gastrointestinal tract. In addition, BiGluc tool can also be used to reliably measure

glucose uptake in animal disease models, such as cancer and can be utilized as a tool for screening of GLUT inhibitors, which is a fast-growing field in cancer drug discovery. Finally, we demonstrated that the sensitivity of our BLI-based method is comparable with the commonly used ^{18}F-FDG-PET tracers, making this novel technology the first successful example of an optical tool for *in vivo* glucose uptake. Our approach substantially broadens the current applications of BLI, extending its potential for imaging glucose and many other small-molecule metabolites that play important roles in human pathologies.

Results

Design and synthesis of bioluminescent probe for measuring glucose uptake (BiGluc)

The recent development of BLI probes to sense molecular signatures of target tissues relies on the simple principle that luciferin "caged" on the phenolic oxygen is not a viable substrate for luciferase until it is uncaged by a specific biological process of interest15, 18. The design strategy for D-glucose mediated bioluminescent signal production is based on a bioorthogonal click reaction (Staudinger ligation)19 between a properly tuned activatable caged luciferin triarylphosphine ester and an azido-modified glucose molecule that results in release of free luciferin, triggering production of quantifiable bioluminescence signal in the presence of firefly luciferase (Fig.1, Supplementary Video 1). When glucose uptake was evaluated *in vitro*, the cells were first incubated with caged luciferin triphenylphosphine (CLP), which is internalized via passive diffusion (Supplementary Fig. 1), washed, and subsequently incubated with the GAz4 reagent (Fig. 1a). To measure glucose uptake *in vivo*, the animals were injected with the CLP reagent (i.v.) 24 h prior to the administration of GAz4 via i.p. injection or oral gavage (o.g.) followed by real-time signal acquisition (Fig. 1b). Importantly, the light production is proportional to the amount of GAz reagent taken up inside the cells or tissue and directly reflected the activity of GLUT transporters.

In order to identify a GAz compound that would possess significant reactivity with CLP probe and also preserve the specificity to the native glucose transporters (GLUTs), we synthesized a series of reagents with an azide substitution of the 2-hydroxy group – a substitution that had been successfully utilized in the design of the ^{18}F-FDG and 2-NBDG glucose probes20 (Fig. 1c). Synthetic procedures and chemical characterizations of novel GAz glucose analogs are described in details in Supplementary Notes 1 and 2. All of the GAz derivatives differ in steric hindrance and electron density around the azide. While a kinetic analysis of the reaction between CLP and GAz1, GAz2 and GAz5 demonstrated low reaction rates, GAz3 and GAz4 provided a three and five orders of magnitude ($x10^5$) enhancement of reaction rate respectively (Fig. 1c). Therefore, GAz4 was used for further *in vitro* and *in vivo* validation studies.

Imaging and quantification of D-glucose uptake in living cells using the BiGluc probe

In order to test whether the new probe could produce light in live cells and if the resulting signal is D-glucose selective, we measured the amount of BiGluc light production from three different cell lines stably transfected with luciferase (4T1-luc, HT1080-luc, and C2C12-luc) under different conditions. First, we determined that incubation of cells with 10 μM of CLP for one hour, followed by a wash and subsequent treatment with 100 μM of the GAz4

reagent results in the highest signal-to-background ratio (Supplementary Fig. 2). Second, we showed that both GAz4 reagent and CLP are not toxic to cells, and do not perturb cellular proliferation in the concentration range used in the assay (Supplementary Fig. 3). Third, GAz4 does not alter cellular redox potential and has no effect on the total NAD^+ concentration (Supplementary Fig. 4). Lastly, we investigated cross-reactivity of GAz4 with naturally occurring thiols such as free cysteine and glutathione. No detectable reduction products were observed for the duration of the test (up to 60 min, Supplementary Fig. 5).

We then investigated whether the resulting light output from the BiGluc probe in living cells was D-glucose specific using a series of competition experiments that have been previously used for testing the behavior of reported glucose probes6, 10, 14. Real-time light production from the BiGluc probe was measured in competition with both D-glucose and the non-natural stereoisomer L-glucose as a negative control in the same cell lines as before (4T1-luc, HT1080-luc, and C2C12-luc). Figure 2a shows that the total light output from the BiGluc probe decreased significantly as the concentration of D-glucose in the buffer increased. At the same time, the signal was not affected by the increasing concentration of L-glucose (Fig. 2b). These results were consistent in all three cell types, demonstrating a direct correlation between D-glucose uptake and light production from the BiGluc probe *in vitro*.

In the next step, we investigated the specificity of the D-glucose signal by directly inhibiting GLUT transporters with cytochalasin B, a potent endofacial inhibitor of the glucose transporter family21. First, we utilized a radioisotope-based assay to validate that the treatment of 4T1-luc cells with cytochalasin B indeed induced GLUT inhibition. As expected, incubation of 4T1-luc cells with 10 μM of cytochalasin B for 10 min resulted in a 23% decrease in radioactive signal (Supplementary Fig. 6a). We then repeated the same cytochalasin B inhibition experiment using the BiGluc probe in two different cell lines (4T1-luc and HT1080-luc) followed by quantification of the bioluminescent signal. The results obtained were in agreement with the radioactive assay and demonstrated 18% and 40% of the signal reduction for 4T1-luc and HT1080-luc, respectively (Supplementary Fig. 6b), further suggesting a direct correlation between bioluminescent light output from the BiGluc probe and D-glucose uptake. Next, we compared the performance of BiGluc with a commercially available GB2-Cy3 probe22. Treatment of 4T1-luc cells with exofacial inhibitor of GLUT transporter 4,6-O-ethylidene-α-D-glucose (4,6-EDG) resulted in decrease of the signal from GB2-Cy3 probe (9%, Supplementary Fig. 6c). We also observed a somewhat more significant bioluminescent signal decrease with BiGluc probe (25%, Supplementary Fig. 6d).

We further explored whether a specific knockout of the GLUT1 transporter known to be overexpressed in many types of cancer23 would influence signal production from the BiGluc probe. We performed CRISPR/Cas9-mediated GLUT1 gene knockout in 4T1-luc cells to produce a GLUT1-deficient version of this cell line (referred as "$GLUT1^{-/-}$"). The knockout was validated by western blot and sequencing that confirmed introduction of mostly frameshift indels, resulting in a functional 'knockout' of the gene (Supplementary Fig. 7). Incubation of the 4T1-luc-$GLUT1^{-/-}$ #1 cells with the BiGluc probe demonstrated a significantly reduced light output (40%) compared to the control (Fig. 2c, Supplementary

Fig. 8a). Next, glucose uptake studies in parental cells, negative control and knockout clones confirmed the results of clone validation (Supplementary Fig. 8b). To further confirm the direct correlation between the BiGluc signal and the activity of GLUT transporters, we performed shRNA-mediated GLUT1 knockdown in 4T1-luc cells. As expected, it resulted in 40-50% reduction in glucose uptake as measured by BiGluc probe (Supplementary Fig. 8c-d).

Since skeletal muscles and adipocytes are known to exhibit insulin-dependent regulation of GLUT4 translocation to the plasma membrane24, we analyzed the effect of PI3K-dependent insulin stimulation on light production using the BiGluc probe. We investigated the performance of the probe in differentiated C2C12 myotubes that were stably overexpressing luciferase (C2C12-luc). C2C12-luc differentiation was confirmed by western blot analysis (Supplementary Fig. 9). As expected, a 32% increase in signal was observed in insulin-treated C2C12-luc cells as compared to the non-insulin treated control (Fig. 2d). In the presence of wortmannin, an inhibitor of PI3K25, the signal elevation was completely suppressed (Fig. 2d). To confirm wortmannin-induced PI3K inhibition, we performed an immunoblot analysis of treated C2C12-luc cells using antibodies directed against AKT, a known PI3K downstream target. AKT phosphorylation levels are insulin-dependent and were abolished upon wortmannin treatment (Fig. 2e). In addition, we tested performance of BiGluc probe using adipocytes differentiated from 3T3-L1 fibroblasts. We observed three times increase in signal intensity upon insulin stimulation (Supplementary Fig. 10) which was fully consistent with previous reports26–28. These results further demonstrate the D-glucose uptake specificity of the BiGluc signal.

To further investigate whether the novel BLI-based probe could provide reliable information on D-glucose uptake *in vitro*, we compared the light output resulting from the BiGluc probe with that of the radioisotope (tritium-labeled glucose,^{3}H-2DG) and fluorescent-based (2-NBDG) probes under the same experimental conditions. In this experiment, C2C12-luc cells were treated with various concentrations of insulin (0-200 nM) followed by incubation with three different reagents (BiGluc, ^{3}H-2DG, and 2-NBDG) and signal acquisition. The results exhibited a linear increase in signal with increasing concentrations of insulin for both BiGluc and ^{3}H-2DG that was expected due to the insulin-dependent GLUT4 translocation to the plasma membrane24. While the radioisotope-based method demonstrated higher sensitivity, the BiGluc approach was equally reliable because the z' factors (a well-known indicator of assay reliability29) for both assays were higher than 0.5 (Supplementary Fig. 11). On the other hand, the fluorescent-based approach using 2-NBDG failed to produce an insulin-dependent increase in signal under these experimental conditions. These data are in agreement with previously published work that reported a poor sensitivity with 2-NBDG readouts in comparison to ^{3}H-2DG for measuring glucose uptake6, 30. Taken together, the results demonstrate that the light production from the BiGluc probe is specific to the GLUT transporter activity and can be used as a reliable, non-invasive, and non-radioactive method to measure D-glucose uptake in live cells.

Imaging and quantification of D-glucose uptake in transgenic reporter mice (FVB-luc$^{+/+}$) using the BiGluc probe

To establish the efficacy of the BiGluc probe for *in vivo* applications, we utilized a genetically engineered mouse model that ubiquitously expresses luciferase through beta-actin promoter (FVB-luc$^{+/+}$ mice) 31. To investigate the clearance of CLP probe from the blood in order to avoid non-specific extra-cellular reaction between CLP and GAz4, we measured bioluminescent signal from the mice intravenously (i.v.) injected with CLP compound. We observed significant ($4x10^3$ fold) drop in signal by 24 h post-injection of CLP which was consistent with significant decrease of CLP plasma concentration measured by HPLC-MS (Supplementary Fig. 12a-b). These results suggest that 24 h is enough for the CLP reagent to clear from the blood and accumulate inside the cells. We found that i.v. administration of CLP 24 h prior to i.p. injection of GAz4 resulted in stable increase in signal up to 1 h followed by 2 h plato (Supplementary Fig. 12c). These results were consistent with signal measured from different organs at 15 and 45 min post injection of GAz4 (Supplementary Fig. 12d).

In the next step, we investigated whether the optical signal produced *in vivo* by the BiGluc probe was D-glucose specific by administering the probe in the presence or absence of high concentrations of D-glucose (competition experiment). The results shown in Figure 3a-c indicate that the competition with D-glucose (1:300 ratio with the GAz4 probe) resulted in suppression of the BiGluc signal to the background level (CLP alone), demonstrating successful competition of BiGluc probe with natural substrate.

To further investigate the D-glucose selectivity of the BiGluc probe *in vivo*, we performed an insulin tolerance test. High levels of insulin should result in GLUT4 translocation to the cellular membrane and a subsequent increase in D-glucose uptake by the tissues32. FVB-luc $^{+/+}$ mice received an i.v. injection of CLP followed by an i.p. injection of the GAz4 reagent 24 h later, either in pure PBS (control) or in combination with insulin, followed by signal acquisition. Remarkably, we observed a three-fold increase in signal for the mice pre-treated with insulin compared to the control group (Fig. 3d). Together, these results demonstrate that the BiGluc probe can be used to reliably quantify physiological fluxes of D-glucose in live animals in a non-invasive fashion.

Imaging and quantification of D-glucose uptake in tumor xenograft models using the BiGluc probe

Glucose transporters, especially GLUT1, play a critical role in the development of several types of cancer33. Therefore, novel reagents that would allow the non-invasive imaging and quantification of GLUT activity in live animals are of high value. To investigate the performance of the BiGluc probe in tumors, we inoculated Swiss nu/nu mice with either 4T1-luc or 4T1-luc-GLUT1$^{-/-}$ #1 (the same cells previously used for *in vitro* experiments; Fig. 2c). The tumors were grown to an average volume of 65 mm^3. All the animals were initially injected with an equimolar dose of luciferin to ensure that the tumor size and level of luciferase expression were equal between the groups. Like the previous *in vivo* experiments, the mice received an i.v. injection of the CLP probe followed by an i.p. injection with the GAz4 reagent 24 h later. The animals were anesthetized, and the light

output was quantified continuously for 1 h. Noticeably, the signal from the mice implanted with 4T1-luc-GLUT1$^{-/-}$ #1 tumors demonstrated a 38% decrease in the total photon flux compared to the control group (Fig. 4a-b) which was consistent with the previous *in vitro* assays results (Fig. 2c). A postmortem analysis of the excised tumors by western blot and immunohistochemistry confirmed the effective deletion of GLUT1 in 4T1-luc-GLUT1$^{-/-}$ #1 tumors (Supplementary Fig. 13a-b).

We also investigated whether the BiGluc signal could be directly modulated through the chemical inhibition of GLUT1 transporters *in vivo*. WZB-117 is a small molecule reversible inhibitor of GLUT1 that is known to efficiently block glucose transport in diverse cancer models34. Nude mice were inoculated with 4T1-luc cells and grown to a volume of about 65 mm^3. The mice from two groups (n = 4) received i.v. injections of CLP followed by an i.p. injection of GAz4 24 h later in either PBS alone (control group) or WZB-117 in PBS (WZB-117 group). We observed a 50% reduction in signal from the group of tumor xenografts from mice treated with the GLUT1 inhibitor (Fig. 4c, d). Notably, no difference in signal production was observed from control group of mice administered with luciferin alone in the presence or absence of WZB-117 (Supplementary Fig. 13c). These results further confirm selectivity of BiGluc signal production from D-glucose uptake in animal models of cancer.

Direct comparison of BiGluc and ^{18}F-FDG-PET in tumor xenograft models

To investigate the performance of the BiGluc probe in comparison to the commonly used clinical techniques, we performed ^{18}F-FDG PET/CT imaging on live mice transplanted with either 4T1-luc cells or 4T1-luc-GLUT1$^{-/-}$ #1 cells (n = 10). We observed that the 4T1-luc-GLUT1$^{-/-}$ #1 tumors exhibited a significantly lower overall uptake of ^{18}F-FDG compared to the 4T1-luc tumors (Fig. 4e, f). This observation was further confirmed by the quantification of the maximum standard uptake value (SUVmax) (Fig. 4e). Like previous experiments, the tumor sizes were equally matched between mice with 4T1-luc and 4T1-luc-GLUT1$^{-/-}$ #1 tumors, demonstrating that the reduction in ^{18}F-FDG uptake in 4T1-luc-GLUT1$^{-/-}$ #1 tumors was not the result of a reduced tumor volume (Supplementary Fig. 13d).

In previously reported studies, GLUT1 transporter expression directly correlated with ^{18}F-FDG uptake in tumors *in vivo*35. To confirm the deletion of the GLUT1 transporter, we performed immunohistochemistry (IHC) staining to measure the GLUT1 expression levels on both 4T1-luc and 4T1-luc-GLUT1$^{-/-}$ #1 tumors. We found significantly lower GLUT1 protein levels in the 4T1-luc-GLUT1$^{-/-}$ #1 tumors compared to their controls (Supplementary Fig. 14a). Interestingly, we identified two mice in the 4T1-luc-GLUT1$^{-/-}$ #1 group that had elevated ^{18}F-FDG uptake (Supplementary Fig. 14b). IHC staining of these tumors showed increased GLUT1 protein expression levels (Supplementary Fig. 14c). We think that the likely explanation why two of the tested 4T1-GLUT1 $^{-/-}$ tumors displayed elevated GLUT1 levels is due to the selection pressure on the tumor, which could revert a single mutation in one allele 36. Overall, these results demonstrate that the BiGluc technique performs very similarly to the gold standard technique in the field of *in vivo* glucose uptake imaging such as ^{18}F-FDG/PET.

Europe PMC Funders Author Manuscripts

Discussion

Glucose plays a key role in cellular metabolism and its uptake has been closely linked to metabolic adaptation in various pathological conditions, such as cancer, diabetes and obesity1–3. However, easily accessible non-invasive *in vivo* imaging techniques for studies of glucose uptake are limited4. Here we describe a new tool to visualize glucose uptake based on non-invasive bioluminescent imaging which is a very sensitive and quantitative modality15–17. The overall approach is based on the combination of caged luciferin technology and the bioorthogonal “click” reaction between an organic azide and appropriately tuned triarylphosphine esters (Staudinger ligation)19. Although the Staudinger ligation is one of the most efficient reactions in living animals37, it has slow kinetics that significantly limits its application for *in vivo* imaging38. We introduced a perfluorophenyl azide moiety in the structure of corresponding azido-glucose derivative (GAz4) increasing the electron withdrawing properties of the azido-modified glucose reagent. This chemical tuning allowed the GAz4 probe to produce a robust bioluminescent signal upon reaction with the CLP both *in vitro* and *in vivo*.

To demonstrate the selectivity of the BiGluc probe towards glucose uptake in living cells, we performed a series of cell-based assays. The results from the D- and L-glucose competition studies successfully demonstrated the concentration-dependent BiGluc signal reduction from D-glucose-treated cells while no change in signal was observed in L-glucose treated controls. To further investigate whether the light output from the BiGluc probe was depended on GLUT1 activity, we performed selective CRISPR/Cas9-mediated GLUT1 gene knockout in 4T1 breast cancer cells stably transfected with luciferase to produce the GLUT1-deficient cell line (4T1-luc-GLUT1$^{-/-}$ #1). Comparison of the signal output from the BiGluc probe between 4T1-luc-GLUT1$^{-/-}$ #1 and 4T1-luc cells established a direct correlation between the light production and GLUT1-mediated glucose uptake. In addition, we performed shRNA-mediated GLUT1 knockdown in 4T1-luc cells. As expected, it resulted in 40-50% reduction in glucose uptake as measured by BiGluc probe. The results of the knockout experiments were in full agreement with the data obtained from cells treated with different exofacial and endofacial GLUT inhibitors where significant reduction in BiGluc signal was observed. Importantly, the magnitude of signal reduction was consistent with previously reported data35, 39, 40.

To further validate the technology, we compared the light output from BiGluc probe in insulin-stimulated adipocytes. The results indicated significant increase in signal upon stimulation with insulin which is again consistent with the previous reports41, 42. Importantly, we also demonstrated that BiGluc probe recapitulated the known PI3K-dependent insulin-induced glucose uptake and can thus be used to measure important physiologically-relevant processes in living cells.

In order to directly compare our novel BiGluc approach with other commonly used methods to measure glucose uptake in living cells, we performed side-by-side experiments where insulin-treated C2C12-luc myotubes were incubated with three different reagents (BiGluc, ^{3}H-2DG, and 2-NBDG). Our results indicate that the BiGluc method is equally reliable compared to the ^{3}H-2DG-approach and superior to that of 2-NBDG. Interestingly, the

BiGluc probe was shown to be more sensitive than previously reported GB2-Cy3 reagent, which could be explained by significantly smaller modifications of D-glucose structure of GAz4 in comparison to rather bulky GB2-Cy3 dye22.

Inspired by these exciting *in vitro* results, we tested the application of the BiGluc probe for the non-invasive imaging of glucose uptake *in vivo*. The selectivity of the BiGluc probe towards glucose uptake *in vivo* was confirmed by competition experiments with high concentrations of D-glucose and insulin stimulation experiments in transgenic reporter mice (FVB-luc$^{+/+}$). To demonstrate the application of the BiGluc technology in cancer models, we evaluated the performance of the probe in mice bearing xenograft tumors of 4T1-luc and 4T1-luc GLUT1 knockouts (4T1-luc GLUT1$^{-/-}$ #1). There are several reports in literature that describe successful tumor formation of GLUT1 KO tumor43, 44. As expected, we observed significant decrease in signal production from BiGluc in GLUT1-knockout mice in comparison to 4T1-luc controls. In addition, we validated application of the BiGluc tool for the identification of novel GLUT1 inhibitors *in vivo*. In this experiment, mice bearing 4T1-luc breast cancer xenografts were injected with a small molecule inhibitor of GLUT1 that is known to efficiently block glucose transport in diverse cancer models (WZB-117)34. The light output resulting from BiGluc probe in WZB-117 treated mice was significantly lower than in the vehicle treated controls further suggesting direct correlation between light production and activity of GLUT transporters. Finally, direct comparison of the performance of the BiGluc probe with ^{18}F-FDG-PET in the same animal model established an identical performance between both reagents. Taken together, the data revealed robust non-invasive detection of physiologically relevant changes of glucose uptake in the animal model of cancer. To the best of our knowledge, this is the first example of an optical imaging reagent that is suitable for non-invasive longitudinal imaging of glucose uptake both *in vitro* and *in vivo*.

Our findings demonstrate the utility of the BiGluc probe as a powerful tool for studies of glucose uptake in living organisms. Many animal models currently exist that express luciferase in various organs or particular tissues like tumors16, 17. Since glucose plays a key role in many human pathological conditions, we believe that this technology can be widely used for drug discovery and for monitoring the development and progression of diseases linked to aberrant glucose uptake such as cancer, diabetes, and obesity1–3. In addition, the BiGluc technology expands the niche of biomolecules that can be probed by bioluminescence. Since other small molecule metabolites can be chemically labeled with azido precursors, this technology represents a powerful new platform for the non-invasive longitudinal imaging of many important metabolites.

Methods

Chemical reagents

Procedures for chemical synthesis and characterization of novel reagents are summarized in Supporting information (SI). All chemical reagents obtained from commercial suppliers were used without further purification unless noted. All compounds/solvents were obtained from Sigma-Aldrich except D-luciferin, which was aquired from Promega.

Europe PMC Funders Author Manuscripts

Cell cultures

All the cell lines used in this study were stably transfected with the luciferase gene. C2C12-luc cells were transfected with firefly luciferase gene and were kindly provided by the lab of Prof. Patrick Aebischer (EPFL, Lausanne, Switzerland). Cells were cultured in DMEM (Gibco) supplemented with 10% fetal bovine serum (FBS) and 1% penicillin-streptomycin (P/S). Myogenic differentiation was initiated upon the cells reaching confluence by switching to a medium containing 2% horse serum. The cells were assayed four days post-confluency. 4T1-luc cells were obtained from (PerkinElmer, Alameda, CA) and transfected with RedLuc luciferase construct. 4T1-luc cells were maintained in RPMI media supplemented with 10% FBS and 1% P/S. HT-1080-luc cells were obtained from (PerkinElmer, Alameda, CA) and were transfected with Luc2 luciferase gene. The cells were grown in minimal MEM supplemented with 10% FBS and 1% P/S. The cells were stably transfected with luciferase gene construct bearing lentivirus (PerkinElmer, CLS960002) and referred here as HT1080-luc cells. 3T3 L1-luc fibroblasts (ATCC) were cultured in DMEM containing 10% fetal calf serum and 1% P/S. Cells were seeded with the density of 2000-3000 cells/cm^2, and split at 60% density to avoid differentiation. To induce pre-adipocyte differentiation, 2 day post-confluent cells were incubated in differentiation medium (DMEM containing 10% FBS, 1% P/S, 1 μg/ml insulin, 0.25 μM dexamethasone, 0.5 mM IBMX and 2 μM rosiglitazone) for 2 days before switching to post-differentiation medium (DMEM containing 10% FBS, 1% P/S and 1 μg/ml of insulin) for additional 2 days. Adipocytes were maintained in DMEM supplemented with 10% FBS and 1% P/S and assayed between 8 and 12 days after initiation of the differentiation. All cells were maintained at 37 °C in a 5% CO_2 atmosphere. In all washing experiments PBS sterile solution was utilized (Thermo Fisher). All cells were maintained at 37°C in a 5% CO_2 atmosphere.

Imaging and quantification of D-glucose uptake in living cells using the BiGluc probe

Cells were plated in a black 96-well plate (4 x 10^4 cells/well) with a clear bottom and assayed the next day or upon differentiation (C2C12-luc, 3T3-L1-luc). For experiments, the growth medium was removed and 10 μM of CLP in Krebs-Ringer-HEPES buffer (KRH; 50 mM of HEPES, 137 mM of NaCl, 4.7 mM of KCl, 1.85 mM of $CaCl_2$, 1.3 mM of $MgSO_4$, 0.1% bovine serum albumin (BSA), pH = 7.4) or KRH alone was added to the buffer in the wells for one hour. Upon incubation, the plates were rinsed twice with phosphate buffered saline (PBS) and replaced with 100 μL of the GAz4 probe in KRH buffer or 10 μM of D-Luciferin in PBS with or without the GAz4 probe, followed by signal acquisition. To investigate signal to background noise ratio, cells were treated with various concentrations of GAz4 in PBS ranging from 5–500 μM (Supplementary Fig. 2). Immediately after addition of GAz4 the plates were imaged using IVIS Spectrum (PerkinElmer, USA) continuously for 30 min. Bioluminescence was quantified using region of interest (ROI) analysis of the individual wells, and the average signal, expressed as the total number of photons emitted per second per cm^2 per steradian (p/sec/cm^2/sr), from each of the wells was calculated using the Living Image 3.2 software (PerkinElmer). Total luminescence was calculated by integrating the area under corresponding kinetic curves. The results were adjusted to the mean relative luciferin signal in all cases when treatment with certain compound (ex.

Europe PMC Funders Author Manuscripts

cytochalasin B) affected luciferase expression. All the uptake measurements were done in triplicate.

In vitro competition and inhibition assays

4T1-luc, HT1080-luc, and C2C12-luc cells were grown as described above (see "Cell culture" section for more details). The medium was removed, and the culture plates were rinsed twice with PBS. The cells were then incubated at 37 °C with 10 μM of CLP in 100 μL of KRH buffer for one hour. Upon incubation, the plates were rinsed twice with PBS followed by the addition of 100 μM of GAz4 with or without either D-glucose or L-glucose at 5 mM and 10 mM in KRH buffer. The cells were immediately placed in the IVIS Spectrum System, and the plates were imaged for 30 minutes continuously, with one image acquired every minute. The appropriate luciferin controls were done in parallel with competition experiments to take into account effect of experimental conditions (addition of D- and L-glucose) on luciferase expression. Briefly, 4T1-luc, HT1080-luc, and C2C12-luc cells were rinsed with PBS followed by the addition of 10 μM of luciferin with or without either D-glucose or L-glucose at 5 mM and 10 mM in KRH buffer.

To examine the effect of cytochalasin B (endofacial inhibitor), WZB-117, and 4,6-EDG (exofacial inhibitor), HT1080-luc and 4T1-luc cells were incubated with 10 μM of CLP as described above, followed by washing with PBS. The cells were then pre-incubated with 10 μM of cytochalasin B for 10 minutes, 50 μM of WZB-117 for 30 minutes and 50 mM of 4,6-EDG for 30 minutes followed by the addition of 100 μM of GAz4 in KRH buffer. The cells were imaged for 30 minutes continuously with one image acquired every minute (IVIS Spectrum, Perkin Elmer USA). The controls included uptake in the absence of an inhibitor and Luciferin. To take into account effects of cytochalasin B on expression levels of luciferase in both cell lines, the same experiment was repeated using luciferin as a control (10 μM in KRH buffer).

Glucose uptake in 4T1-luc cells inhibited with 4,6-EDG was also measured with commercially available fluorescent probe, GB2-Cy3 (Spark Biopharma, Korea). Protocol for inhibition is described above followed by addition of 100 μM of GB2-Cy3 in KRH buffer. The cells were incubated with the probe fore 30 min followed by rinsing with cold PBS (x3). The fluorescence signal was acquired immediately with the imager (IVIS Spectrum, Perkin Elmer USA) with a Cy3 channel.

Measurement of D-glucose uptake in insulin-stimulated differentiated myotubes and adipocytes (C1C12-luc, 3T3-L1-luc)

Bioluminescent light production from BiGluc probe was measured in C2C12-luc and 3T3-L1 cells upon their complete differentiation and compared to their non-differentiated controls. Prior to probe incubation, the cells were starved in serum-free growth medium overnight before treatment with insulin. The cells were washed with KRH buffer and incubated with 10 μM of CLP with or without 100 nM of insulin in KRH buffer for 1 h, followed by rinsing with PBS (x2) and subsequent addition of 100 μM of GAz4 in KRH buffer. The bioluminescence signal was acquired immediately every minute for 30 minutes continuously. The controls included measurement of BiGluc light production by non-

stimulated cells. All the results were adjusted to the mean relative signal obtained from cells treated with luciferin control (10 μM) with and without insulin.

Glucose uptake in insulin-stimulated differentiated myotubes was also measured with commercially available fluorescent probe, 2-NBDG. Protocol for insulin stimulation is described above followed by addition of 300 μM of 2-NBDG in KRH buffer. The cells were incubated with the probe fore 30 min followed by rinsing with PBS (x2). The fluorescence signal was acquired immediately on a plate reader (TECAN) with excitation at 475 nm and emission at 550 nm, as suggested by the reagent provider.

Measurement of D-glucose uptake in the PI3K-dependent pathway with BiGluc probe

Differentiated C2C12-luc cells were incubated for 30 minutes at 37°C in a humidified 5% CO_2 atmosphere in medium containing 100 nM of wortmannin, then washed with PBS and co-stimulated with 100 nM of insulin and 10 μM of CLP in KRH buffer for 30 minutes. Upon incubation, the cells were washed with PBS followed by the addition of 100 μM of GAz4 in KRH. The cells were immediately imaged for 30 minutes continuously, with one image acquired every minute. The cells incubated with media lacking wortmannin were used as a positive control. As described above the results were normalized to the mean relative signal from control cells treated with luciferin (10 μM).

2-deoxy-D-[^{3}H] (^{3}H-2DG) glucose uptake in insulin dose-dependent assay

The stimulatory activity of insulin in glucose transport was analyzed by measuring the cell uptake of ^{3}H-2DG. Differentiated C2C12-luc cells grown in 24-well plates were washed twice with serum-free DMEM and incubated with 0.5 ml of the same medium at 37°C overnight. The cells were washed three times with KRH buffer and incubated with insulin in different concentrations ranging from 0–200 nM for 30 minutes. Glucose uptake measurements was initiated by the addition of 55.5 MBq/l of ^{3}H-2DG and 1 mmol/l of regular glucose, as the final concentrations. After 20 minutes, the experiment was terminated by washing the cells three times with cold PBS, and cell lysing with RIPA buffer (50 mM Tris HCl, 150 mM NaCl, 1 % Triton X–100, 0.5 % Na-deoxycholate, 0.1 % SDS). The radioactivity retained by the cell lysates was measured by an LS 6000 Series Liquid Scintil (Beckman Coulter, U.S.).

CRISPR/Cas9-mediated GLUT1 knockout in 4T1-luc cells

CRISPR/Cas9-mediated GLUT1 knockout in 4T1-luc cells was done according to the manufacturer's instructions (Santa Cruz Biotechnology, Inc). Briefly, 5 x 10^4 cells were plated onto 12-well microplates and allowed to grow to 70 % confluence. Next, 20 μg of GLUT1 CRISPR/Cas9 KO Plasmid (sc-422998) was added to 4 μL of UltraCruz Transfection Reagent (sc-395739). The complexes were incubated for 20 minutes and then overlaid onto the cells. The plates were incubated at 37°C in a 5% CO_2 for 72 hours. Transfected cells were sorted based on GFP fluorescence using a FACSDiva cell sorter from Beckton Dickinson (U.S.) to sort one cell per well into 96-well plates (two plates per batch of transfected cells). The cells were cultured in RPMI with 10% FBS and 1% P/S, and after 14 days, GFP-expressing colonies were determined by inspection under a microscope equipped with UV light. Expanded-sorted cell populations were phenotypically analyzed to

confirm complete allelic knockout. The Control CRISPR/Cas9 Plasmid (sc-418922) contained non-targeted 20-nucleotide scrambled guide RNA (gRNA), not recognizing any DNA sequence and therefore not binding or cleaving genomic DNA, was designed as a negative control.

PCR amplification and sequencing of *Slc2a1* amplicons

DNA from 4T1-luc cells, the CRISPR/Cas9 clones knockouts (KO) and their negative controls (NC) was isolated using NucleoSpin® Tissue Kit (Macherey-Nagel, Germany) according to the manufacturer's instructions. Primers that amplified 200- to 400-bp regions surrounding the sites of interest (C region (exon 3) and AB region (exon 5) of *Slc2a1* gene) were selected using the program Geneious Prime (Supplementary Notes 3). Genomic loci were amplified with Taq polymerase (BioLabs, US) using 50 ng of genomic DNA as input. PCR products were cloned into the pCR™4-TOPO® cloning vector according to the manufacturer's instructions (Invitrogen Corporation, CA). The TA cloning reactions were transformed by heat shock into DH5α™ competent cells (Invitrogen Corporation, CA). DNA from ten colonies for each clone was extracted using the QIAprep® Spin Miniprep Kit (Qiagen, Germany) and sequenced at Microsynth with the company's M13F primer. Sequences were analyzed using Geneious prime (https://www.geneious.com).

shRNA knockdown

pLKO.1-shRNA-GLUT1#1(Mission TRC shRNA, TRCN0000079328), shRNA-GLUT1#2 (Mission TRC shRNA, TRCN0000311403), shRNA-GLUT1#3 (Mission TRC shRNA, TRCN0000324209), shRNA-GLUT1#4 (Mission TRC shRNA, TRCN0000305719) and shRNA-GLUT1#5 (Mission TRC shRNA, TRCN0000079332) plasmids were obtained from Sigma. For lentivirus production, HEK 293 TN cells were transfected with pLKO.1 shRNA-GLUT1 along with standard packaging plasmids by calcium transfection. Hygromycin-resistant 4T1-luc cells were incubated with viral supernatant containing 4 mg/ml polybrene. Selection of transduced cells was then performed with 5 mg/mL of puromycin. Targeting sequences for all shRNA are provided in Supplementary Notes 4.

Western blot analysis

Protein lysates were prepared by lysing cells in RIPA buffer containing protease inhibitor cocktail. The protein concentration was determined using the BCA protein assay (Thermo Scientific), and 30 μg of proteins were separated by SDS-PAGE and transferred to a 0.2 mm nitrocellulose membrane. The membranes were blocked by tris-buffered saline (TBS; 0.2 M Tris base, 1.5 M NaCl), 0.1% Tween-20, and 5% ECL blocking reagent (GE Healthcare) for one hour, then incubated with the primary antibody, GLUT1 (Abcam, ab15309), GLUT4 (Santa Cruz, sc-53566), Akt (Cell Signaling, #9272), P-Akt (Cell Signaling, #9271), heavy chain myosin (Abcam, ab124205) or glycogen synthase (Cell Signaling, #3893). Then, the membranes were incubated with HRP-conjugated secondary antibody (Abcam) diluted in TBS with 0.1% Tween-20. After the addition of the HRP substrate, the chemiluminescent signal was detected using a Gel and Blot Imaging System (Azure Biosystems). The same membrane was stripped and reused for detection of β-actin (Abcam, ab8229) or α-Tubulin (Sigma, #T6074) as a loading control, following the same protocol as above.

Cytotoxicity and cell viability assay

Cytotoxicity assays were carried out using a one-step fluorometric assay based on the use of AlamarBlue (Invitrogen). 4T1-luc cells were incubated with a broad concentration range of the GAz4 probe (50 nM – 50 mM) for one and 24 hours followed by three hours of incubation with AlamarBlue in 96-well microplates at 37°C in a 5% CO_2 atmosphere. Upon incubation, the fluorescence of the AlamarBlue was read on a plate reader (TECAN) with excitation at 530 nm and emission at 590 nm.

Cell viability was calculated as a percentage of viable cells and normalized to DMF only control. Cells were incubated with either GAz4 (100 μM) or CLP (10 μM) for varying time intervals (24, 48, and 72 h) at 37 °C and 5% CO_2 (bottom graph in every panel). The intensity of chemiluminescence was measured by ELISA kit according to manufacturer's instructions (Abcam, ab126572). Results presented as a mean of 3 independent experiments.

NAD^+ assay

NAD^+ was extracted from cells and measured by EnzyChrom NAD/NADH Assay Kit (BioAssay Systems) according to manufacturer's instructions.

Experimental animals

We purchased FVB-$luc^{+/+}$ (full abbreviation: FVB-Tg[CAG-luc,-GFP]L2G85Chco/J) mice from Jackson Laboratory and Swiss nu/nu mice from Charles River Labs. All animal bioluminescent imaging experiments were reviewed and approved through a license 2849 from the Swiss Cantonal Veterinary Office Committee for Animal Experimentation according to the Swiss National Institutional Guidelines. PET imaging animal studies were approved by the University of California Los Angeles (UCLA, USA) Animal Research Committee and were carried out according to the guidelines of the Department of Laboratory Medicine at UCLA.

Imaging and quantification of D-glucose uptake in transgenic reporter mice (FVB-$luc^{+/+}$) using the BiGluc probe

24 h prior the imaging, 3 groups of FVB-$luc^{+/+}$ mice (n = 3), were pretreated with 100 μL of 1.5 mM CLP reagent dissolved in PBS with 0.1% BSA and fasted for 12 hours. The next day the first group was given oral gavage of 100 μL of PBS (control group); the second group was gavaged with 100 μL of GAz4 reagent in PBS in a dose of 12 mg/kg; the third group received oral gavage of GAz4 reagent in a dose of 12 mg/kg in PBS mixed with D-glucose at 1.6 g/kg). The mice were imaged immediately using CCD camera (IVIS Spectrum, PerkinElmer, U.S) by acquiring images every minute for one hour continuously. The resulting data was analyzed using the Living Image software taking the area of the entire body as region of interest (ROI).

Insulin tolerance test

FVB-luc+/+ mice (n = 4) were intravenously injected 100 μL of 1.5 mM CLP reagent dissolved in PBS with 0.1% BSA. 20 h post CLP injection the mice were fasted for 4 h followed by 15 min imaging session using CCD camera (IVIS Spectrum, PerkinElmer, U.S)

to aquire background signal. The mice were then intraperitoneally (i.p.) injected with either solution of GAz4 in a dose of 12 mg/kg or GAz4 in a dose of 12 mg/kg mixed with insulin solution at the final concentration of 0.1 U/ml in PBS. The mice were imaged immediately using CCD camera by acquiring images every minute for one hour continuously. The resulting data were analyzed using the Living Image software taking the area of the entire body as the region of interest (ROI).

CLP clearance study

Mice were i.v. injected with 100 μL of 1.5 mM CLP reagent dissolved in PBS with 0.1% BSA. After administration of CLP or vehicle (PBS) the blood was collected via heart puncture at three different time points (0, 8, and 24 hours) into tubes containing Heparin. Plasma was separated by centrifugation at 2000 rpm for 5 min at 4 °C. GAz4 in the final concentration of 1mM was added to plasma samples, so the residual CLP could react and produce free luciferin. Next, plasma was added to the cells expressing luciferase (4T1-luc) that were used as a bioluminescent reporter to quantify the amount of free luciferin. Bioluminescence was measured for 30 min using IVIS Spectrum (PerkinElmer, USA). The total photon flux from cells was normalized to 1 μM of D-luciferin control to account for different cell number.

Imaging and quantification of D-glucose uptake in tumor xenograft models using the BiGluc probe

Imaging of 4T1-luc and 4T1-luc-GLUT1$^{-/-}$ xenografts—4T1-luc and 4T1-luc-GLUT1$^{-/-}$ #1were harvested, washed twice in PBS, and resuspended in 100 μL of serum-free RPMI before being inoculated subcutaneously to the dorsal side of the Swiss nude mice (n=5) at approximately 1 million cells/mouse. Tumors were measured twice a week, and when the tumor volume reached 65 mm^2 the mice were administered 1.5 mM of CLP dissolved in 100 μL PBS containing 0.1% BSA via i.v. injection. After 24 hours, the mice received i.v. injections of GAz4 (12 mg/kg in 100 μL PBS). The mice were anesthetized with isoflurane, and the bioluminescence was acquired immediately every minute for one hour using the auto-exposure mode. The following day the mice were imaged again upon injection of luciferin (15 mg/mL, 100 μL in PBS) and imaged for 30 min to assure equal light production between the group and control for tumor size. Upon imaging, mice were sacrificed, and the corresponding tumors were dissected for further examination by histological analysis (Supplementary Fig. 15).

Imaging of 4T1-luc xenografts treated with WZB-117 inhibitor—4T1-luc cells were harvested, washed twice in PBS, and resuspended in 100 μL of serum-free RPMI before being inoculated subcutaneously to the dorsal side of the Swiss nude mice (n=4) at approximately one million cells/mouse. Tumors were measured twice a week, and when the tumor volume reached 65 mm^2, the mice were administered 1.5 mM of CLP dissolved in 100 μL PBS containing 0.1% BSA via i.v. injection. Similar to the previous experiment, the first group received i.v. injections of GAz4 (12 mg/kg in 100 μL PBS) 24 h post CLP injection. The second group was injected i.p. with WZB-117 (10 mg/kg in PBS/DMSO (1:1, v/v)) one hour prior to administration of GAz4. Both groups were imaged for the duration of 1 hour using IVIS Spectrum camera (PerkinElmer, USA). The following day the mice were

imaged again upon i.p. injection of luciferin (15 mg/mL, 100 μL in PBS) and imaged for 30 min. The total phone flux obtained from each mouse imaged with BiGluc probe was normalized to the signal produced upon i.p. injection of equimolar amounts of luciferin (100 μM in 100 μL of PBS) to control for tumor size.

In a separate experiment (n=4) we performed measurements of light production from mice that received i.p. injection of luciferin (15 mg/mL, 100 μL in PBS) with and without WZB-117 inhibitor. Similar to experiment described above, one group of mice was injected i.p. with WZB-117 (10 mg/kg in PBS/DMSO (1:1, v/v)) one hour prior to administration of luciferin. No difference in signal was observed.

PET Imaging

In vivo small animal imaging was conducted at the Crump Institute's Preclinical Imaging Technology Center, UCLA, USA. Mice underwent microPET (GENISYS 8 PET/CT, Sofie Biosciences) and microCT (CrumpCAT, Arion Hadjioannou laboratory) imaging with ^{18}F-fluorodeoxyglucose (^{18}F-FDG). Briefly, mice were injected via the lateral tail vein with radiolabeled probe (70 μCi for ^{18}F-FDG) then underwent 60-minute uptake under 2% isoflurane anesthesia, followed by static microPET and microCT imaging. The microPET images were acquired for 600 seconds with an energy window of 150–650 keV, reconstructed using maximum-likelihood expectation maximization with corrections for photon attenuation, detector normalization, and radioisotope decay (scatter correction was not applied), and converted to units of percent injected dose per gram (%ID/g). The microCT images were acquired under "high resolution" continuous mode using a 50 kVp, 200 μA X-ray source and were reconstructed using the Feldkamp algorithm with a voxel size of 125 μm. ROI analysis was conducted using AMIDE version 1.0.545 on tumors and select normal tissues (liver, muscle, lung, heart, brain, and subcutaneous fat). To account for overall PET probe biodistribution variations between animals, tumor uptake was normalized to the liver for ^{18}F-FDG, as previously described46.

Immunohistochemistry

The tumors were excised and fixed for 16 hours in 10% buffered formalin. The tissues were processed and embedded by the Translational Pathology Core Laboratory (TPCL) at UCLA. Slides were stained following published protocols47. Briefly, following deparafinization, antigen retrieval was performed by the heat-induced antigen retrieval method following the manufacturers' suggestions for each antibody. Endogenous peroxidase activity was quenched by incubating the slides in 3% hydrogen peroxide for 10 minutes. Blocking was completed with 5% goat serum for one hour at room temperature. Following incubation with the primary GLUT1 antibody (Alpha Diagnostics # GT11-A) and secondary antibody, avidin-biotin peroxidase (ABC) complex (Vector Labs) was used. Finally, staining was visualized using the ImmPACT DAB (Vector Labs). Slides were counterstained with dilute hematoxylin. Following IHC staining, slides were digitally scanned onto a ScanScope AT (Aperio Technologies, Inc.), and images were captured.

Europe PMC Funders Author Manuscripts

Statistical analysis

Statistical analysis was carried out in GraphPad Prism 8.0.2. Quantitative data are presented as mean ± SD, if not stated otherwise. Differences were compared using the Student's t-test. When p values were 0.05 or less, the differences were considered statistically significant.

Reporting summary

Further information on research design is available in the Nature Research Reporting Summary linked to this paper.

Supplementary Material

Refer to Web version on PubMed Central for supplementary material.

Acknowledgements

We thank Leenaards Foundation, NCCR Chemical Biology, and Swiss National Foundation (grant number CR23I3_157023) for generous financial support. We thank the laboratory of P. Aebischer for the kind gift of C2C12-luc cells. We thank the laboratory of D. Fescher and A. Stahl for the kind gift of HEK 293 TN and 3T13-L1 cells, respectively. We thank J. Frigell for the synthesis of several GAz derivatives (data not shown). We thank A. Konovalova for performing initial *in vitro* experiments on GAz probes (data not shown). We also thank P. Gonschorek and B. Mangeat for help with analyzing sequences. We also thank the laboratory of K. Sakamoto for kind gift of GLUT4 antibodies. We thank EPFL core facilities for histology, MS, and NMR analysis (in particular P. Mieville and E. Baudat for technical support).

References

1. Hay N. Reprogramming glucose metabolism in cancer: can it be exploited for cancer therapy? Nature reviews. Cancer. 2016; 16:635–649. [PubMed: 27634447]
2. Kaur J. A Comprehensive Review on Metabolic Syndrome. Cardiology Research and Practice. 2014; 2014:21.
3. Chang C-H, Pearce EL. Emerging concepts in immunotherapy – T cell metabolism as a therapeutic target. Nature immunology. 2016; 17:364–368. [PubMed: 27002844]
4. Momcilovic M, Shackelford DB. Imaging Cancer Metabolism. Biomolecules & therapeutics. 2018; 26:81–92. [PubMed: 29212309]
5. Cox BL, Mackie TR, Eliceiri KW. The sweet spot: FDG and other 2-carbon glucose analogs for multi-modal metabolic imaging of tumor metabolism. American journal of nuclear medicine and molecular imaging. 2015; 5:1–13. [PubMed: 25625022]
6. Hu F, et al. Vibrational Imaging of Glucose Uptake Activity in Live Cells and Tissues by Stimulated Raman Scattering. Angewandte Chemie. 2015; 54:9821–9825. [PubMed: 26207979]
7. Kim WH, Lee J, Jung DW, Williams DR. Visualizing sweetness: increasingly diverse applications for fluorescent-tagged glucose bioprobes and their recent structural modifications. Sensors (Basel, Switzerland). 2012; 12:5005–5027.
8. Vallabhajosula S, Solnes L, Vallabhajosula B. A broad overview of positron emission tomography radiopharmaceuticals and clinical applications: what is new? Seminars in nuclear medicine. 2011; 41:246–264. [PubMed: 21624560]
9. Tseng JC, Wang Y, Banerjee P, Kung AL. Incongruity of imaging using fluorescent 2-DG conjugates compared to 18F-FDG in preclinical cancer models. Molecular imaging and biology : MIB : the official publication of the Academy of Molecular Imaging. 2012; 14:553–560. [PubMed: 22302178]
10. O'Neil RG, Wu L, Mullani N. Uptake of a fluorescent deoxyglucose analog (2-NBDG) in tumor cells. Molecular imaging and biology : MIB : the official publication of the Academy of Molecular Imaging. 2005; 7:388–392. [PubMed: 16284704]

11. Speizer L, Haugland R, Kutchai H. Asymmetric transport of a fluorescent glucose analogue by human erythrocytes. Biochimica et biophysica acta. 1985; 815:75–84. [PubMed: 4039191]
12. Cheng Z, et al. Near-infrared fluorescent deoxyglucose analogue for tumor optical imaging in cell culture and living mice. Bioconjugate chemistry. 2006; 17:662–669. [PubMed: 16704203]
13. Kovar JL, Volcheck W, Sevick-Muraca E, Simpson MA, Olive DM. Characterization and performance of a near-infrared 2-deoxyglucose optical imaging agent for mouse cancer models. Analytical biochemistry. 2009; 384:254–262. [PubMed: 18938129]
14. Park J, Lee HY, Cho MH, Park SB. Development of a cy3-labeled glucose bioprobe and its application in bioimaging and screening for anticancer agents. Angewandte Chemie. 2007; 46:2018–2022. [PubMed: 17285672]
15. Mezzanotte L, van 't Root M, Karatas H, Goun EA, Lowik C. In Vivo Molecular Bioluminescence Imaging: New Tools and Applications. Trends in biotechnology. 2017; 35:640–652. [PubMed: 28501458]
16. Dothager RS, et al. Advances in bioluminescence imaging of live animal models. Current opinion in biotechnology. 2009; 20:45–53. [PubMed: 19233638]
17. Genevois C, Loiseau H, Couillaud F. In Vivo Follow-up of Brain Tumor Growth via Bioluminescence Imaging and Fluorescence Tomography. International journal of molecular sciences. 2016; 17:1815.
18. Li J, Chen L, Du L, Li M. Cage the firefly luciferin! - a strategy for developing bioluminescent probes. Chemical Society reviews. 2013; 42:662–676. [PubMed: 23099531]
19. Saxon E, Bertozzi CR. Cell Surface Engineering by a Modified Staudinger Reaction. Science. 2000; 287:2007–2010. [PubMed: 10720325]
20. Sundhoro M, Jeon S, Park J, Ramstrom O, Yan M. Perfluoroaryl Azide Staudinger Reaction: A Fast and Bioorthogonal Reaction. Angewandte Chemie. 2017; 56:12117–12121. [PubMed: 28796447]
21. Estensen RD, Plagemann PGW, Cytochalasin B. Inhibition of Glucose and Glucosamine Transport. Proceedings of the National Academy of Sciences of the United States of America. 1972; 69:1430–1434. [PubMed: 4338593]
22. Park J, et al. Impact of molecular charge on GLUT-specific cellular uptake of glucose bioprobes and in vivo application of the glucose bioprobe, GB2-Cy3. Chemical communications (Cambridge, England). 2014; 50:9251–9254.
23. Yun J, et al. Glucose deprivation contributes to the development of KRAS pathway mutations in tumor cells. Science. 2009; 325:1555–1559. [PubMed: 19661383]
24. Cushman SW, et al. Molecular mechanisms involved in GLUT4 translocation in muscle during insulin and contraction stimulation. Advances in experimental medicine and biology. 1998; 441:63–71. [PubMed: 9781314]
25. Eguez L, et al. Full intracellular retention of GLUT4 requires AS160 Rab GTPase activating protein. Cell metabolism. 2005; 2:263–272. [PubMed: 16213228]
26. Capilla E, et al. Functional characterization of an insulin-responsive glucose transporter (GLUT4) from fish adipose tissue. American Journal of Physiology-Endocrinology and Metabolism. 2004; 287:E348–E357. [PubMed: 15113704]
27. Nedachi T, Kanzaki M. Regulation of glucose transporters by insulin and extracellular glucose in C2C12 myotubes. American Journal of Physiology-Endocrinology and Metabolism. 2006; 291:E817–E828. [PubMed: 16735448]
28. Maeda N, et al. Diet-induced insulin resistance in mice lacking adiponectin/ACRP30. Nat Med. 2002; 8:731. [PubMed: 12068289]
29. Zhang JH, Chung TD, Oldenburg KR. A Simple Statistical Parameter for Use in Evaluation and Validation of High Throughput Screening Assays. Journal of biomolecular screening. 1999; 4:67–73. [PubMed: 10838414]
30. Blodgett AB, et al. A fluorescence method for measurement of glucose transport in kidney cells. Diabetes technology & therapeutics. 2011; 13:743–751. [PubMed: 21510766]
31. Cao YA, et al. Shifting foci of hematopoiesis during reconstitution from single stem cells. Proceedings of the National Academy of Sciences of the United States of America. 2004; 101:221–226. [PubMed: 14688412]

32. Saltiel AR, Kahn CR. Insulin signalling and the regulation of glucose and lipid metabolism. Nature. 2001; 414:799–806. [PubMed: 11742412]
33. Szablewski L. Expression of glucose transporters in cancers. Biochimica et biophysica acta. 2013; 1835:164–169. [PubMed: 23266512]
34. Ojelabi OA, Lloyd KP, Simon AH, De Zutter JK, Carruthers A. WZB117 (2-Fluoro-6-(m-hydroxybenzoyloxy) Phenyl m-Hydroxybenzoate) Inhibits GLUT1-mediated Sugar Transport by Binding Reversibly at the Exofacial Sugar Binding Site. The Journal of biological chemistry. 2016; 291:26762–26772. [PubMed: 27836974]
35. Goodwin J, et al. The distinct metabolic phenotype of lung squamous cell carcinoma defines selective vulnerability to glycolytic inhibition. Nature communications. 2017; 8
36. Chavez A, et al. Precise Cas9 targeting enables genomic mutation prevention. Proceedings of the National Academy of Sciences. 2018; 115:3669.
37. Shah L, Laughlin ST, Carrico IS. Light-Activated Staudinger-Bertozzi Ligation within Living Animals. Journal of the American Chemical Society. 2016; 138:5186–5189. [PubMed: 27010217]
38. Sletten EM, Bertozzi CR. Bioorthogonal chemistry: fishing for selectivity in a sea of functionality. Angewandte Chemie. 2009; 48:6974–6998. [PubMed: 19714693]
39. Liu Y, et al. A small-molecule inhibitor of glucose transporter 1 downregulates glycolysis, induces cell-cycle arrest, and inhibits cancer cell growth in vitro and in vivo. Molecular cancer therapeutics. 2012; 11:1672–1682. [PubMed: 22689530]
40. Suzuki S, et al. Involvement of GLUT1-mediated glucose transport and metabolism in gefitinib resistance of non-small-cell lung cancer cells. Oncotarget. 2018; 9:32667–32679. [PubMed: 30220973]
41. Maeda N, et al. Diet-induced insulin resistance in mice lacking adiponectin/ACRP30. Nat Med. 2002; 8:731–737. [PubMed: 12068289]
42. Yun H, et al. Inulin increases glucose transport in C2C12 myotubes and HepG2 cells via activation of AMP-activated protein kinase and phosphatidylinositol 3-kinase pathways. Journal of medicinal food. 2009; 12:1023–1028. [PubMed: 19857065]
43. Young CD, et al. Modulation of glucose transporter 1 (GLUT1) expression levels alters mouse mammary tumor cell growth in vitro and in vivo. PloS one. 2011; 6:e23205–e23205. [PubMed: 21826239]
44. Wellberg EA, et al. The glucose transporter GLUT1 is required for ErbB2-induced mammary tumorigenesis. Breast cancer research : BCR. 2016; 18:131–131. [PubMed: 27998284]
45. Loening AM, Gambhir SS. AMIDE: a free software tool for multimodality medical image analysis. Molecular imaging. 2003; 2:131–137. [PubMed: 14649056]
46. Venneti S, et al. Glutamine-based PET imaging facilitates enhanced metabolic evaluation of gliomas in vivo. Science translational medicine. 2015; 7
47. Momcilovic M, Shackelford DB. Targeting LKB1 in cancer - exposing and exploiting vulnerabilities. British journal of cancer. 2015; 113:574–584. [PubMed: 26196184]

Europe PMC Funders Author Manuscripts

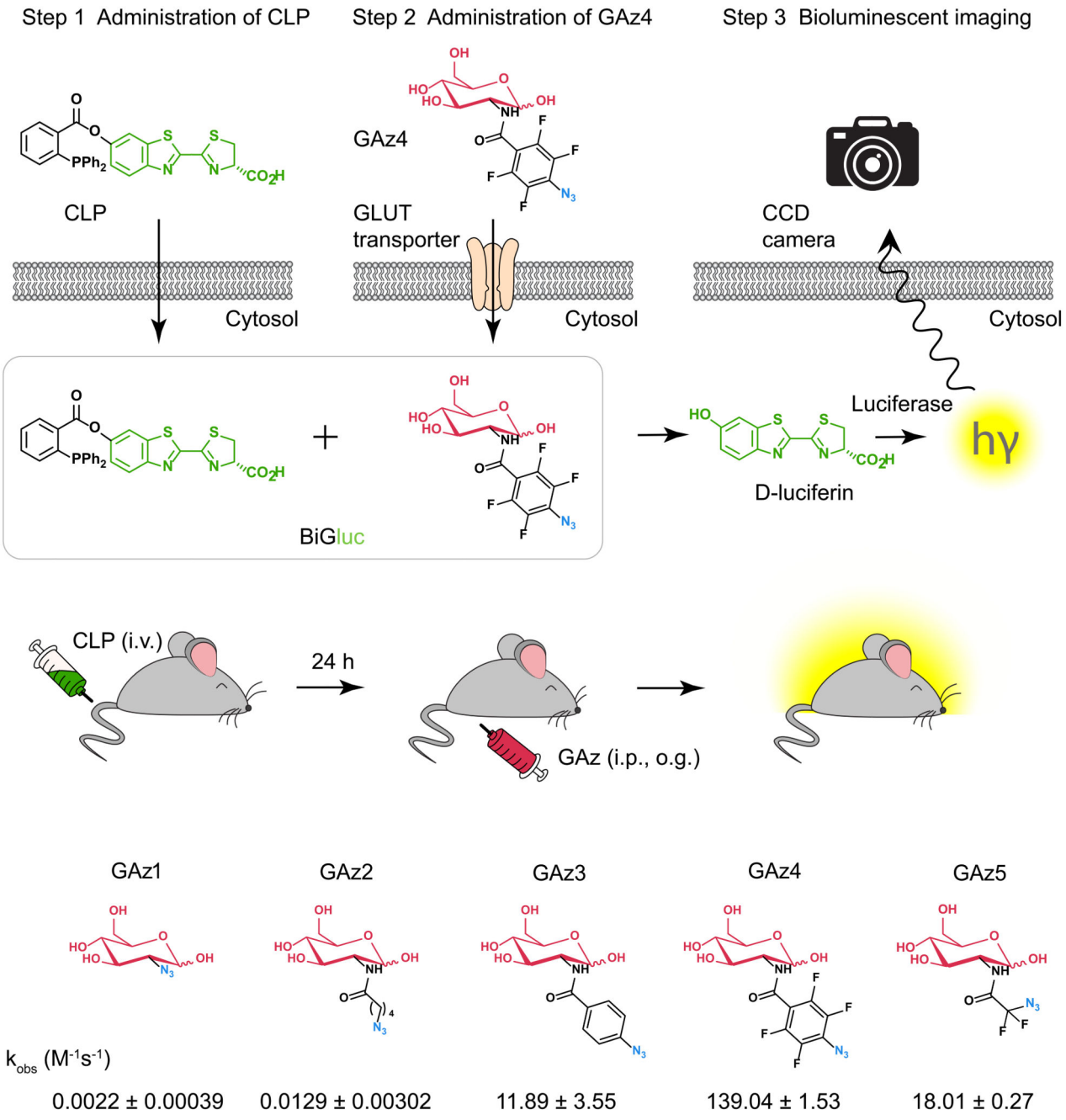

Figure 1. Design strategy for D-glucose bioluminescent probe (BiGluc).

(a) Schematic representation of the *in vitro* application of BiGluc technology. The technology is based on the biorthogonal reaction (Staudinger ligation). Two reagents, "caged luciferin phosphine" (CLP) and "glucose azide" (GAz), undergo a reaction inside the cell resulting in the release of free luciferin, which is subsequently processed by luciferase to produce flux of light. Hence, the light output is proportional to the amount of GAz4 reagent taken up inside the cells and is quantified using a CCD camera or plate reader. **(b)** BiGluc method is suitable for *in vivo* application. Animals expressing luciferase are first injected

with CLP and after 24 h they are administered with GAz4. Immediately after GAz4 administration, animals are monitored using camera imaging system to quantify light produced upon reaction of BiGluc components inside cells. **(c)** Structures of the synthesized azido-glucoses (GAz1-GAz5) investigated for the best reactivity with CLP reagent in the Staudinger ligation reaction. Reaction rate constants are presented as Mean ± SEM (n = 3, independent experiments).

Europe PMC Funders Author Manuscripts

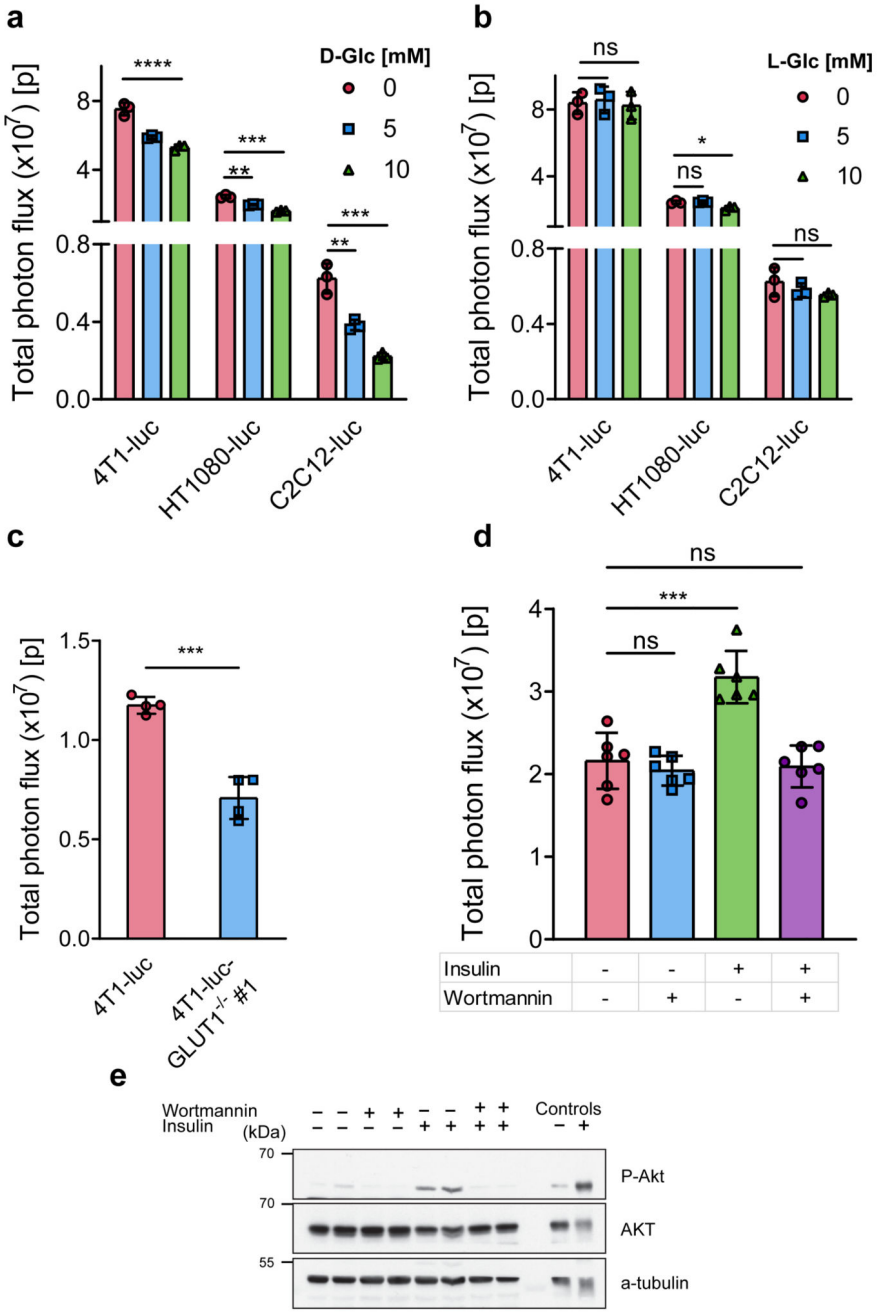

Figure 2. Imaging and quantification of D-glucose uptake in living cells using the BiGluc probe.

(a) Total photon flux obtained from BiGluc probe in 3 different cell lines stably transfected with luciferase construct (4T1-luc, HT1080-luc, and C2C12-luc). The cells were first incubated for one hour with CLP, washed with PBS, and then treated with GAz4 in the presence or absence of the natural competitor D-glucose (0, 5, and 10 mM) followed by signal acquisition. Bars represent area under the curve (total photon flux) over 20 minutes (n = 3). **(b)** same as **(a)**, but D-glucose was replaced with L-glucose in identical concentrations (0, 5, and 10 mM) (n = 3). **(c)** Comparison of light production using BiGluc probe in 4T1-

Europe PMC Funders Author Manuscripts

luc and GLUT1 knockout 4T1-luc cells (4T1-luc and 4T1-luc- GLUT1$^{-/-}$ #1 respectively, n = 4). The experiment was performed as described in **(a)**. **(d)** Total photon flux from C2C12-luc myotubes treated with 10 μM wortmannin for 30 minutes and 100 nM insulin for 30 minutes as outlined in the table, followed by the addition of BiGluc probe as described in **(a)** and signal acquisition (n = 6). **(e)** Western blot analysis of the phosphorylation status of Akt in C2C12-luc cells using the treatment described in the table. The total photon flux from cells was normalized to the appropriate luciferin control in cases where the experimental conditions influenced the signal of luciferin production. Data in **a-d** are presented as mean ± SD, each *n* represents a biologically independent sample. Experiments in **a-e** were performed independently at least twice. *$P < 0.05$, **$P < 0.01$, ***$P < 0.001$, ****$P < 0.0001$, *ns* – non-significant by two-tailed *t* test. For blot source images, see Supplementary Figure 15. For individual P values, see Source Data.

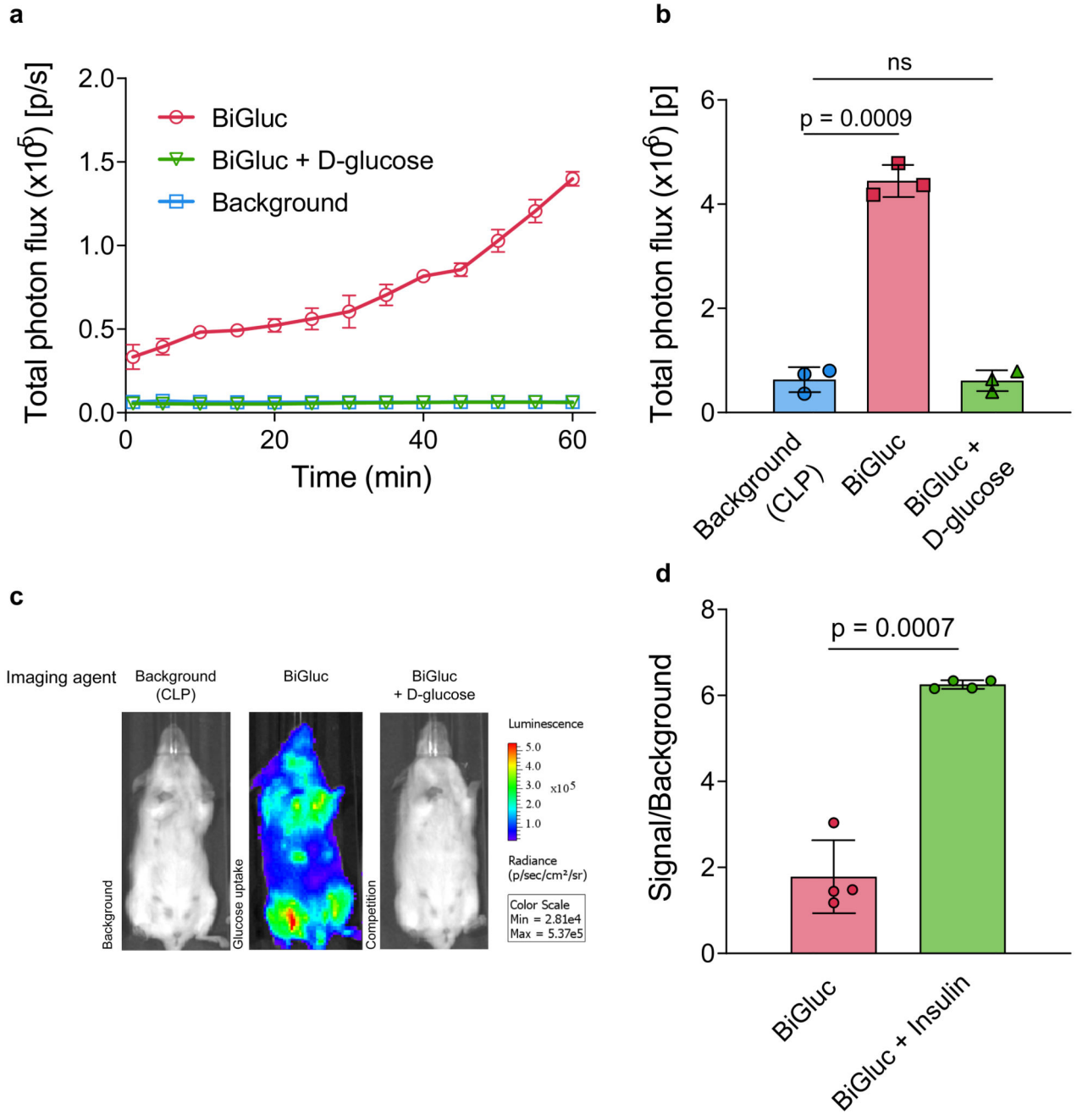

Figure 3. Imaging and quantification of D-glucose uptake in transgenic reporter mice (FVB-luc $^{+/+}$) using the BiGluc probe

(a) Non-invasive quantification of the whole-body bioluminescent signal over time in three different groups of FVB-luc$^{+/+}$ mice (Background, BiGluc, BiGluc plus D-glucose). Mice were first injected i.v. with CLP solution, 24 h later mice received an oral gavage of either GAz4 (BiGluc group), or GAz4 + D-glucose (BiGluc+D-glucose group), or PBS (Background group). Bioluminescent signal acquisition started immediately after the oral gavage to mice (n = 3). **(b**) Integration of the kinetic curves (AUC) shown in **(a)** over 60

minutes (n = 3). Signal to background ratio was 7.5-fold. **(c)** Representative images from the three groups of mice. **(d)** Effect of insulin treatment on glucose uptake measured with BiGluc. FVB-luc$^{+/+}$ mice were intravenously injected CLP. After 24 h they were intraperitoneally (i.p.) injected with either GAz4, or GAz4 plus insulin, followed by 1h of imaging. Signal to background ratio was calculated for each group. Data are presented as mean ± SD (n = 4 per group) Each *n* represents a biologically independent sample. Experiments in **a-d** were performed independently at least twice.

Europe PMC Funders Author Manuscripts

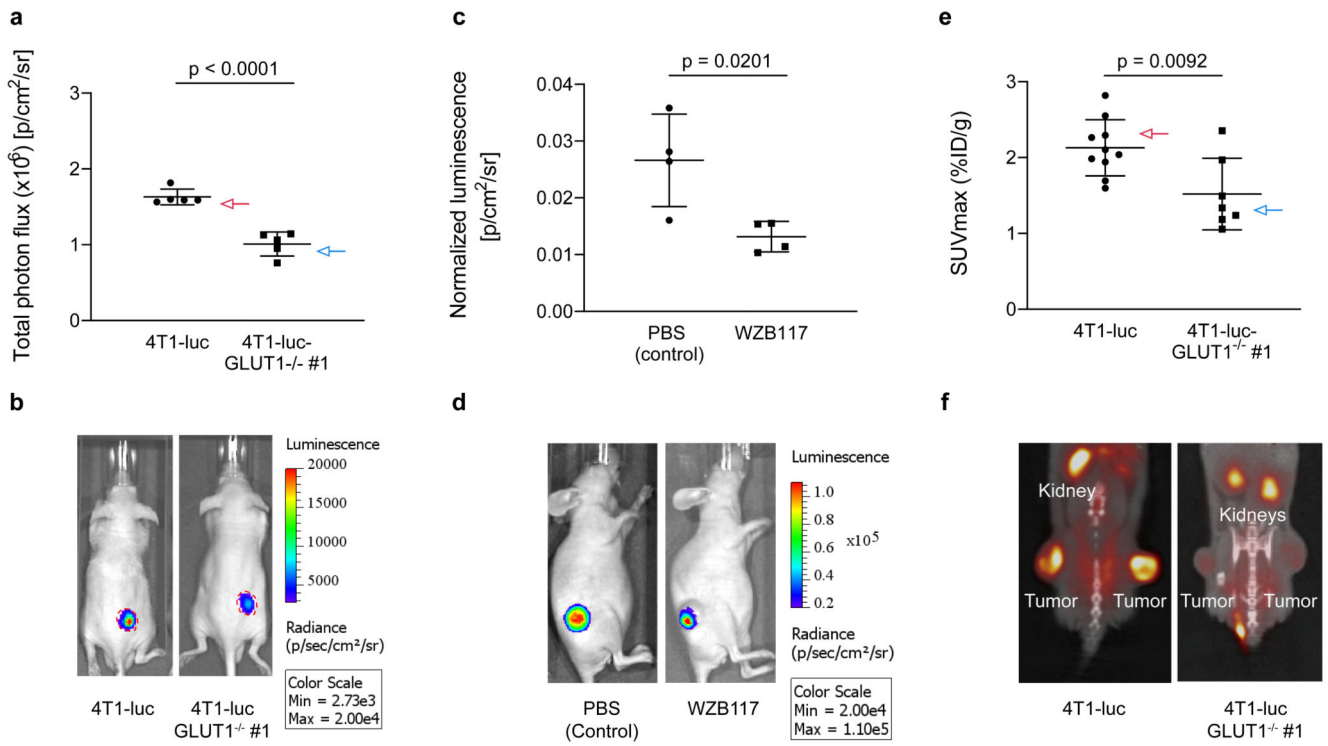

Figure 4. Imaging and quantification of D-glucose uptake in tumor xenograft models using the BiGluc and ^{18}F-FDG probes

(a) Comparison of glucose uptake by subcutaneous tumors formed by 4T1-luc and 4T1-luc-GLUT1$^{-/-}$ #1 cells. The cells were injected into Swiss nu/nu mice subcutaneously and allowed to grow.. When tumors reached 65 mm^2 size, mice received intravenous injections of CLP 24 h prior to i.p. injection of GAz4. A decrease of signal on 38% was observed in the 4T1-luc GLUT1-deficient tumors compared to 4T1-luc controls. Graph represents total photon flux over 10 minutes from xenografts (n = 5). **(b)** Representative images of mice bearing 4T1-luc or 4T1-luc-GLUT1$^{-/-}$ #1 tumors are shown. The red line represents the margin of the tumors indicating similar tumor size in both groups. **(c)** Investigation of BiGluc light output upon treatment with GLUT1 transporter specific inhibitor (WZB-117). Swiss nu/nu mice were injected with 4T1-luc cells. When tumors reached the size of 65 mm^3, the mice were divided in 2 groups (4 animals in each) and were i.v. injected with CLP. 24 h later they received i.p. injection of GAz4 or combination of GAz4 and WZB-117. Graph represents areas under the kinetic curves over 60 minutes normalized to photon flux resulting from equimolar injection of luciferin (n = 4). **(d)** Representative images of mice with and without of inhibitor WZB-117 treatment. **(e)** Glucose uptake by 4T1-luc and 4T1-luc-GLUT1$^{-/-}$ #1 tumors measured by PET. Maximum standard uptake values (SUVmax) were calculated by measuring the percent injected dose (%ID/g) of ^{18}F-FDG in tumors (n = 10, 4T1-luc tumors and n = 7, 4T1-luc-GLUT1$^{-/-}$ #1 tumors). **(f)** Representative images of ^{18}F-FDG PET/CT scans of mice bearing 4T1-luc or 4T1-luc-GLUT1$^{-/-}$ #1 tumors. Data are presented as mean ± SD. *p* values were calculated using two-tailed t-test. Each *n* represents a

Europe PMC Funders Author Manuscripts

biologically independent sample. All experiments were repeated independently at least twice.

Europe PMC Funders Author Manuscripts